Diffusion Monte Carlo Simulations of small Quantum Systems using simple Trial Wave Functions

Denmark, January 2015

Bachelor's Thesis
Submitted by

Kristoffer Vinther Olesen
20116384
Department of Physics and Astronomy
Aarhus University

Supervisor
Dmitri Vladimir Fedorov

Abstract

In this paper we will investigate the diffusion Monte Carlo method for solving the Schrödinger equation numerically. We will give a detailed account for the theoretical background including the fixed node approximation, which is used when calculating fermionic and/or excited states. Hereafter we develop an algorithm capable of preforming basic DMC-simulations on states without nodes and importance sampled DMC-simulations on excited states. Using this algorithm, the energy and wave function of the lowest states of Hydrogen, Helium, H^-, and H_2^+ are calculated with simple trial wave functions. The results are compared with theoretical and experimental data, in order to determine whether simple trial wave function are useful for calculating energies and wave functions with reduced computation time. We find, that simple trial wave function can give a fairly accurate value of the energy, however, will not yield a correct image of the wave function.

Contents

1 Introduction

During the past few decades advances in the processing power of computers have led to a dramatic improvement in our ability to simulate quantum systems. Today the most successful methods are the Quantum Monte Carlo methods. The simplest of these methods are the variational Monte Carlo (VMC) method. This method uses Monte Carlo integration in order to evaluate the expectation values for a given trial wave function. The main drawback of the VMC is that the accuracy of the result depends on the accuracy of the trial wave function. In this theses we utilize another method, the diffusion Monte Carlo method (DMC). In this method the limitations of trial wave functions is overcome, by using a projection method to pick out the ground state component of a starting wave function. The DMC method consists of a random movement of particles in space subject to a probability of multiplication or disappearance. The drawback of the DMC method is that in it's pure form, it is only useful for finding the bosonic ground states. However, using different boundary conditions the method can be generalized to find wave functions for fermionic systems and excited states. These boundary conditions are generally defined by the nodal planes of a guess trial wave functions. The trial wave functions can also be used to bias the random walk by the implementation of importance sampling in order to reduce statistical variation. The goal of all simulation tools is to achieve a high amount of accuracy with a minimal amount of computational cost. Using simple trial wave function instead of optimized wave functions will decrease the computational cost, but how much will it affect the accuracy of the result?

In this thesis we report random walk calculations on few body systems using simple trial wave functions. We begin by outlining the theoretical background of the DMC-method. We will then construct an algorithm capable of preforming a DMC-simulation for few body systems. We will test this algorithm on the atomic Hydrogen and Helium systems before studying the ions H^- and H_2^+.

2 Theory

The structure and physical properties of atoms and molecules are described by a wave function $\Psi(\vec{R},t)$, that is a function of time and the coordinates of all particles expressed as the vector $\vec{R}$. The wave function is the solution to the complex wave equation known as the Schrödinger equation.

$$i\hbar\frac{\delta\Psi(\vec{R},t)}{\delta t} = -\frac{\hbar^2}{2m_e}\nabla^2\Psi(\vec{R},t) + V(\vec{R})\Psi(\vec{R},t) \tag{1}$$

If the physical potential of the system $V(\vec{R})$ is independent of time we can separate the variables and find that solutions can be written on the form.

$$\Psi(\vec{R},t) = \psi_E(\vec{R})e^{-iEt/\hbar} \tag{2}$$

where E is a constant and the functions $\psi_E(\vec{R})$ are called stationary states and satisfy the time-independent Schrödinger equation.

$$E\psi_E(\vec{R}) = -\frac{\hbar^2}{2m_e}\nabla^2\psi_E(\vec{R}) + V(\vec{R})\psi_E(\vec{R}) = H\psi_E(\vec{R}) \tag{3}$$

where we have introduced the Hamiltonian of the system $H = -\frac{\hbar^2}{2m_e}\nabla^2 + V(\vec{R})$. The general solution to the Schrödinger equation is a linear combination of solutions to the time-independent Schrödinger equation.

$$\Psi(\vec{R},t) = \sum_{n=0}^{\infty} c_n \psi_n(\vec{R}) e^{-iE_n t/\hbar} \tag{4}$$

The coefficients c_n describe the overlap between the eigenfunction $\psi_n(\vec{R})$ and the wave function $\Psi(\vec{R},\tau)$.

$$c_n = \int_{-\infty}^{\infty} \psi_n^*(\vec{R})\Psi(\vec{R},t)d\vec{R} = \left\langle \psi_n(\vec{R}) | \Psi(\vec{R},t) \right\rangle$$

In order to describe many electron system, one have to solve the time-independent Schrödinger equation. For a molecular system the Hamiltonian to be used in (3) contains many terms since it must contain the kinetic energy of every particle and also the potential of every particles electronic interaction with the rest. The Hamiltonian has the form.

$$\hat{H} = -\sum_k \frac{1}{2M_k}\nabla_k^2 - \sum_i \frac{1}{2}\nabla_i^2 - \sum_{ik} \frac{Z_k}{\mid \vec{r_k} - \vec{r_i} \mid} + \sum_{k_1 k_2} \frac{Z_{k_1} Z_{k_2}}{\mid \vec{r_{k_1}} - \vec{r_{k_2}} \mid} + \sum_{i_1 i_2} \frac{1}{\mid \vec{r_{i_1}} - \vec{r_{i_2}} \mid} \tag{5}$$

The index k runs over all nuclei and the index i runs over all electrons. The two first terms are the kinetic energy of the nucleus and electron respectively. The third term is the Coulomb potential between the nucleus with charge Z_k and position $\vec{r_k}$ and the electron in position $\vec{r_i}$. The two last terms are the potential of the electronic repulsion between the nuclei and electrons respectively. However, analytical solution of (3) are only possible for few simple Hamiltonians. In general we need to make approximations to simplify the Hamiltonian. One such successful approximation is the Born-Oppenheimer approximation, which states that the motion of the nuclei is much slower compared to the motion of the electrons. This means that the kinetic energy term of the nuclei is removed and that the potential repulsion between the nuclei is constant since the internuclear distance is constant. In this paper we shall examine the numerical method of solving the time-independent Schrödinger equation (3) known as diffusion Monte Carlo. We show it is possible to transform the time dependent Schrödinger equation into an integral equation describing the time evolution. Furthermore we find that in the long time limit the wave function will be dominated by the wave function of the ground state. This is the foundation of the diffusion Monte Carlo method. By approximating the time dependent wave function as a sum of points, it can be evolved through time as a diffusion process.

2.1 Monte Carlo Integration

Monte Carlo Integration is a numerical method of determining definite multidimensional integrals. Consider the integral.

$$I = \int_\Omega f(\vec{x})d\vec{x} \tag{6}$$

, where Ω is a subspace of $\mathbb{R}^N$ with volume.

$$V = \int_\Omega d\vec{x}$$

According to the basic Monte Carlo approach the integral (6) can be approximated by summing the values of $f(\vec{x})$ at N points with a factor of V/N.

$$I \approx \frac{V}{N}\sum_{i=1}^{n} f(\vec{x_i}) \tag{7}$$

The points $\vec{x}_i$ are chosen, so that they are uniformly distributed over Ω. A major advantage of Monte Carlo integration compared to other numerical integration methods, is that the variance of I is independent of the number of dimensions. In addition to this the variance decreases as $1/\sqrt{N}$, making it possible to determine I to any desired accuracy by simple increasing the amount of points chosen. The variance can be deceased even further by implementing importance sampling. Instead of sampling the points $\vec{x}_i$ from a uniform distribution, they are sampled from a non-uniform probability density $p(\vec{x})$ which shape resembles that of the integrand on the subspace Ω. By doing this, we have to weigh the more common points less than the uncommon points and the approximation of (6) becomes.

$$I \approx \frac{1}{N} \sum_{i=1}^{N} \frac{f(\vec{x}_i)}{p(\vec{x}_i)} \tag{8}$$

2.2 Imaginary Time Schrödinger Equation

If we define imaginary time as $\tau = i \cdot t$ and introduce an arbitrary shift in energy E_R, from now on referred to as the reference energy, the Schrödinger equation in atomic units takes the form:

$$-\frac{\delta \Psi(\vec{R}, \tau)}{\delta \tau} = -\frac{1}{2}\nabla^2 \Psi(\vec{R}, \tau) + (V(\vec{R}) - E_R)\Psi(\vec{R}, \tau) \tag{9}$$

The imaginary time Schrödinger equation is similar to an ordinary diffusion equation modified by a branching term. The solution to the Schrödinger equation can be written as a linear combination of the stationary states and their characteristic exponential time dependence.

$$\Psi(\vec{R}, \tau) = \sum_{n=0}^{\infty} c_n \psi_n(\vec{R}) e^{-(E_n - E_R)\tau} \tag{10}$$

The eigenfunctions $\psi_n(\vec{R})$ and their respective eigenvalues E_n are obtained from the time independent Schrödinger equation.

$$\hat{H}\psi_n(\vec{R}) = E_n \psi_n(\vec{R}) \tag{11}$$

The exponential time dependence in (10) depends on the value of the reference energy. If the $E_R > E_n$ the exponential diverges and if $E_R < E_n$ the exponential dies off. However, if $E_R = E_n$ the exponential equals unity. This means that if the reference energy equals the energy of the ground state, an evolution of the wave function in imaginary time will be dominated by the ground state after a sufficiently long time, since all excited states have higher energy than the ground state.

$$\lim_{\tau \to \infty} \Psi(\vec{R}, \tau) = c_0 \psi_0(\vec{R}) \tag{12}$$

We now need a way to evolve the wave function in imaginary time for some reference energy. We saw that the reference energy need to equal the ground state energy, however this is of cause unknown from the beginning. We therefore also need some way to change our reference energy continuously in order to make sure the wave function converges to the ground state.

By setting a function $G(\vec{R}, \vec{R}', d\tau)$ as the probability for an electron to move from a position $\vec{R}$ to $\vec{R}'$ during the short timespan $d\tau$, the short time evolution of the wave function can be calculated by the integral.

$$\Psi(\vec{R}', \tau + d\tau) = \int_{-\infty}^{\infty} G(\vec{R}, \vec{R}', d\tau)\Psi(\vec{R}, \tau) d\vec{R} \tag{13}$$

The transition probability $G(\vec{R}, \vec{R}', d\tau)$ can be thought of as a wave function of an electron at position $\vec{R}$ at time τ and at position $\vec{R}'$ at time $\tau + d\tau$. Therefore $G(\vec{R}, \vec{R}', d\tau)$ must also satisfy the imaginary Schrödinger equation. If the second term of the imaginary Schrödinger equation is neglected, (9) is simply an ordinary diffusion equation in $3N$ dimensions, N being the number of electrons, and the solution is a simple Gaussian function with mean $\vec{R}$ and variance $d\tau$. The transition probability is then.

$$G_d = \left(\frac{1}{2\pi d\tau}\right)^{-3N/2} e^{-\frac{(\vec{R}' - \vec{R})^2}{2d\tau}} \tag{14}$$

If the first term is neglected the imaginary Schrödinger equation is a branching equation and has the solution.

$$G_b = e^{-(V(\vec{R}) - E_R)d\tau} \tag{15}$$

The transition probability can be approximated to the second order of $d\tau$ by the product of 14 and 15 [1]. The short time evolution of the wave function then becomes.

$$\Psi(\vec{R}', \tau + d\tau) = \int_{-\infty}^{\infty} \Psi(\vec{R}, \tau) \left(\frac{1}{2\pi d\tau}\right)^{-3N/2} e^{-\frac{(\vec{R}' - \vec{R})^2}{2d\tau}} e^{-(V(\vec{R}') - E_R)d\tau} d\vec{R} \tag{16}$$

In order to obtain the wave function of the ground state we need to evaluate the short time integral (16) enough times for the limit (12) to be valid. In the DMC-algorithm this is done by a series of diffusion processes according to (14) and branching processes according to (15).

2.3 Random Walk Method

In order to use the Monte Carlo methods described earlier when calculating the ground state energy, we need to be able to sample an unknown ground state wave function. However, using the short time evolution integral (16) we can evolve samples from an initial known wave function. Imagine sample points from the wave function $\Psi(\vec{R}', \tau + d\tau)$ is wanted. If we can interpret the wave function as a probability density we can use the Monte Carlo method (8) and the short time evolution integral (16) can be approximated as.

$$\Psi(\vec{R}', \tau + d\tau) \approx \frac{1}{N} \sum_{\substack{i=1 \\ \vec{R}_i \in \Psi(\vec{R}, \tau)}}^{N} \left(\frac{1}{2\pi d\tau}\right)^{-3N/2} e^{-\frac{(\vec{R}' - \vec{R}_i)^2}{2d\tau}} e^{-(V(\vec{R}') - E_R)d\tau} \tag{17}$$

The approximation contains a factor which is a sum of gaussian functions with mean at the sample points of $\Psi(\vec{R}, \tau)$. This factor means that $\Psi(\vec{R}', \tau + d\tau)$ is larger for points within a gaussian function with mean $\vec{R}_i$ and variance $d\tau$. Therefore an appropriate choice of the next sample points would be points normally distributed around each former point. Then each of these new sample points are weighted by the exponential $e^{-(V(\vec{R}') - E_R)d\tau}$. Accumulating these weights after every time step is very computationally heavy, however, instead we can depending on the value of the potential create additional sample points or kill off sample points.

Because the wave function itself is considered as a probability density, meaning that it must be positive definite, the applicability of the DMC-algorithm is limited only to bosonic ground states. This is because only

the absolute value of the square can be interpreted as a probability density according to the general principles of quantum mechanics. It is, however, possible to overcome these limitations by the utilizing the Fixed Node Approximation, (FNA).

An DMC-simulation is begun by sampling an initial wave function $\Psi(\vec{R}, 0)$ at N points, known as walkers, each of which then undergo the described diffusion meaning that each point diffuses to a point given by.

$$\vec{x'} = \vec{x} + \sqrt{d\tau}p \tag{18}$$

Here p is a Gaussian random number with mean 0 and variance 1. If the walkers are points in multiple dimensions they diffuse by (18) in each dimension. After this each walker is subject to a branching process. If the potential energy of the walker is larger than the reference energy, equation (15) is less than unity, and the probability for that walker to disappear becomes.

$$P_D = 1 - e^{-(V(\vec{R})-E_R)d\tau} \tag{19}$$

If the potential energy of the walker is smaller than the reference energy, equation (15) is greater than unity, and the associated probability for that walker to spawn new walkers becomes.

$$P_B = e^{-(V(\vec{R})-E_R)d\tau} - 1 \tag{20}$$

The probability of birth consist of an integer part $m = 0, 1, 2...$ and a fraction f less than unity. After each diffusive step a walker with potential energy less than the reference energy spawns m new walkers identical to the parent walker. Additionally for each initial walker a uniform random number between 0 and 1 is compared to P_D and f and if smaller this walker disappears of spawns an additional walker respectively. The combined diffusion and branching process changes the distribution of the walkers in such a way that the walkers is now distributed according to a probability density identified as $\Psi(\vec{R}, \tau + d\tau)$. This process is then repeated for a large number of times so the limit (12) becomes applicable. A graphical description of the DMC-simulation is given in figure 1. As time progress particles die in regions where the potential is high and multiplies in regions of low potential. In the end the particles will be distributed according to the wave function of the ground state.

Due to the branching process the total number of walkers change. As mentioned earlier the long time limit of the wave function only goes towards the ground state function, (12), if the reference energy equals the ground state energy. If the reference energy is bigger than the energy of the ground state the distribution $\lim_{\tau\to\infty} \Psi(\vec{R}, \tau)$ would diverge i.e. increasing the number of walker through all bounds. If the reference energy is smaller than the energy of the ground state the distribution $\lim_{\tau\to\infty} \Psi(\vec{R}, \tau)$ would go to zero, or killing off all walkers. Only if the reference energy equals the ground state energy the distribution $\lim_{\tau\to\infty} \Psi(\vec{R}, \tau)$ would settle such that the number of walkers will fluctuate around a steady state number, N_0. It is possible to adjust the value of the reference energy after each branching process so that the number of walkers stay approximately constant. This is done by setting.

$$E_R = \langle V \rangle - \frac{N - N_0}{N_0 d\tau} \tag{21}$$

Once the steady state distribution has been reach and the number of particles fluctuate very little around N_0, the reference energy equals the average potential energy of the walkers. By integrating the energy eigenvalue

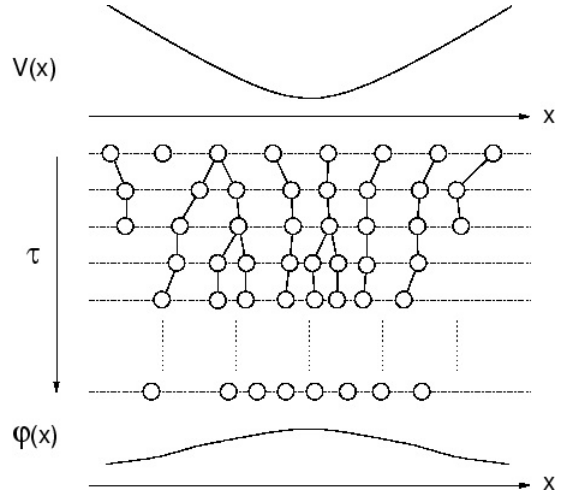

Figure 1: Evolution of walkers in a DMC-simulation. In regions of high potential the walkers dies and in regions of low potential they multiply. Eventually the walkers are distributed according to the ground state wave function.

equation (11) over the entire configuration space we find that the average potential energy also equal the energy expectation value of the distribution $\Psi(\vec{R},\tau)$.

$$\begin{aligned} E_0 \int \Psi(\vec{R},\tau)d\vec{R} &= \int \hat{H}\Psi(\vec{R},\tau)d\vec{R} \\ &= -\frac{1}{2}\int_{\delta\Omega} \nabla\Psi(\vec{R},\tau)d\vec{S} + \int V(\vec{R})\Psi(\vec{R},\tau)d\vec{R} \end{aligned} \tag{22}$$

The divergence theorem has been applied on the first term one the second line. This term vanishes since it describes the walker flow across the boundary and the integration is carried out over the entire configuration space. Since we can think of $\Psi(\vec{R},\tau)$ as a probability density the expectation value becomes.

$$E_0 = \frac{\int V(\vec{R})\Psi(\vec{R},\tau)d\vec{R}}{\int \Psi(\vec{R},\tau)d\vec{R}} \tag{23}$$

This is on a form that is suitable for Monte Carlo integration since the walkers are distributed according to the distribution density $\Psi(\vec{R},d\tau)$. Using the approximation (8) the energy expectation value becomes.

$$E_0 = \frac{1}{N}\sum_{i=1}^{N} V(\vec{R}_i) \tag{24}$$

The main sources for error in a random walk calculation are statistical variations due to the randomness of the calculation procedure and the use of a finite time step, $d\tau$. Any statistical variations can easily be estimated by preforming several calculations on the same quantum system. Errors due to the use of a finite time step stem from the fact that the motions should be continuous, and that the driving function (16) is an approximation which only holds for small $d\tau$. The effects of using a finite time step can be tested be repeating calculations using different time step sizes, and extrapolation the energy to $d\tau = 0$.

2.4 Fixed Node Approximation

As noted the DMC-method depends on the interpretation of the wave function being a distribution density and hence being positive definite. However, wave functions are not generally positive definite. Regions of different sign are needed for fermionic wave functions to be antisymmetric under the interchange of fermions as well as the orthonormality of excited states wave functions. By result the DMC-method is only usefull for finding the bosonic ground state wave functions. The fixed node approximation imposes boundary conditions of the form $\Psi(\vec{R}) = 0$ using the nodes of a reference function as the nodes of the wave function. The DMC-method is the carried out in these regions of constant sign and the wave function evolve to the that of the ground state in each region separately. Any walker that cross the nodes should be killed off in order to ensure the $\Psi(\vec{R}) = 0$ boundary condition. If the nodes of the reference function are the same as the exact wave function the fixed node solution is exact, since in each nodal region the walkers are distributed according to the wave function of the lowest state with the imposed nodes. If, however, the nodes of the reference function are only approximative, then the fixed node solutions obey the variational principle if the wave function in question is a fermionic ground state. For excited states it is possible, due to the birth-death mechanism, for the nodal region with the lowest energy to be overpopulated in the long time limit, and therefore it is possible for excited to calculate a energy lower than the exact energy. This enforces the importance of choosing a good reference function. There are no general procedure of finding the nodal surfaces, but the nodes of functions optimized by Hartree-Fock calculation, variational Monte Carlo, or other variational methods work very well in practice including for excited states. The elimination of walkers crossing the boundaries between the regions does introduce some systematic error in the calculation, since the finite time step in the DMC-method allows for the possibility of walkers crossing a node and recrossing back into the allowed region. Such a walker is not eliminated because it begins and ends in the allowed region, however, it should. The probability of a walker crossing and recrossing a node is a function of the distance from the node at the initial, R, and final position, R'. The probability of moving from an initial position with a distance R from the nodal plane to a position with distance R' from the nodal plane is.

$$P_m = \frac{1}{\sqrt{2\pi d\tau}} e^{-\frac{(R'-R)^2}{2d\tau}} \tag{25}$$

Meanwhile the probability of moving from the initial position to the image of the final position in the nodal plane is.

$$P_i = \frac{1}{\sqrt{2\pi d\tau}} e^{-\frac{(R'+R)^2}{2d\tau}} \tag{26}$$

If a walker steps onto the nodal plane during a finite time step the probability of going to the final position, m, or its image, i, must be equal. Therefore the probability P_i is equal to the probability of moving to position R' by a route crossing and recrossing the nodal plane. The probability of crossing and recrossing the nodal plane given that the move must end in position m, is then the ratio of P_i to P_m

$$P_x = e^{-\frac{2RR'}{d\tau}} \tag{27}$$

After each time step not only walkers which crosses the nodal planes should be eliminated, but also walkers for which the probability P_x exceeds a random number in the interval $]0;1[$.

2.5 Importance Sampling

The efficiency of the discussed DMC-method can be improved by the implementation of importance sampling. Since the Coulomb potential present in atomic and molecular system is inversely proportional to distance, it is possible for the branching term in (9) to diverge leading to large fluctuations in the population and increased statistical errors. By multiplication with a trial wave function, $\Psi_T(\vec{R})$, which we expect to resemble the desired wave function, the imaginary time Schrödinger equation can be rewritten as (see appendix).

$$-\frac{\delta f(\vec{R},\tau)}{\delta\tau} = -\frac{1}{2}\nabla^2 f(\vec{R},\tau) + \nabla(\vec{v}_D f(\vec{R},\tau)) + (E_L(\vec{R}) - E_R) f(\vec{R},\tau) \tag{28}$$

Here we have defined a new distribution, $f(\vec{R},\tau)$, the drift velocity, $\vec{v}_D(\vec{R})$, and the local energy, $E_L(\vec{R})$ as.

$$f(\vec{R},d\tau) = \Psi_T(\vec{R})\Psi(\vec{R},d\tau) \tag{29}$$

$$\vec{v}_D(\vec{R}) = \frac{\nabla\Psi_T(\vec{R})}{\Psi_T(\vec{R})} \tag{30}$$

$$E_L(\vec{R}) = -\frac{\nabla^2\Psi_T(\vec{R})}{2\Psi_T(\vec{R})} + V(\vec{R}) \tag{31}$$

If our trial wave function share the nodes and the signs of the actual wave function we can without loss of generality assume the distribution $f(\vec{R},d\tau)$ to be positive definite, and therefore eligible for the simulation described earlier. A simulation using importance sampling has to be slightly modified in order to incorporate the drift velocity and local energy. Consequently the transition probabilities corresponding to (28) is.

$$G_d = \left(\frac{1}{2\pi d\tau}\right)^{3N/2} e^{-\frac{(\vec{R}' - \vec{R} - d\tau\cdot\vec{v}_D(\vec{R}))^2}{2d\tau}} \tag{32}$$

$$G_b = e^{-(E_L(\vec{R})-E_R)d\tau} \tag{33}$$

The exponential in the diffusion function, (32), now also contains a term dependent on the drift velocity and the branching exponential, (33), now contains the local energy instead of the electronic potential. The sampling procedure described above have to be modified accordingly. In addition to the random diffusion motion each walker now also undergo a drift motion equal to the product of the time step size and the drift velocity, $d\tau\cdot\vec{v}_D(\vec{R})$. This drift motion drives the walkers away from the nodes of the trial wave function, and towards regions where it has a large absolute value. This help enforce the fixed-node approximation. In real simulations it is however still possible for walkers to cross the nodal planes. This is due to the standard deviation of the random diffusion motion being proportional to $\sqrt{d\tau}$ and the directed drift motion being proportional to $d\tau$. Since most simulations use time step sizes less than 1 in order to ensure the approximation of the transition probability (16), it is possible for the diffusion motion to overcome the drift and move across the nodes. Such walkers should either be killed off as discussed previously, or it should be kept in it's original position. Either method is valid, but it turns out rejecting moves crossing nodal planes yield smaller time step

errors compared to killing of walkers [1]. The branching probabilities are also changed when introducing importance sampling. The probabilities of a walker dying or giving birth to new walkers are modified to.

$$P_D = 1 - e^{-(E_L(\vec{R})-E_R)d\tau} \tag{34}$$

$$P_B = e^{-(E_L(\vec{R})-E_R)d\tau} - 1 \tag{35}$$

Using the local energy instead of the potential energy in order to determine the branching probabilities may greatly improve the accuracy of DMC calculations, since the local energy is mostly better behaved than the electronic potential function. If the trial wave function is almost equal the the exact ground state wave function the local energy is nearly constant and equal to the ground state energy so any fluctuations in population will be greatly reduced.

The result of a DMC simulation using importance sampling is walkers distributed according to the mixed state $\Psi_T(\vec{R})\Psi_0(\vec{R})$. Therefore the ground state energy can be calculated using the mixed state estimator [2].

$$E_0 = \frac{\left\langle \Psi_0(\vec{R}) \mid \hat{H} \mid \Psi_T(\vec{R}) \right\rangle}{\left\langle \Psi_0(\vec{R}) \mid \Psi_T(\vec{R}) \right\rangle} \tag{36}$$

$$= \frac{\int E_L(\vec{R}) f(\vec{R},\tau) d\vec{R}}{\int f(\vec{R},\tau) d\vec{R}} \tag{37}$$

This integral is on a form capable for Monte Carlo integration. Using (8) the energy of the ground state is.

$$E_0 = \frac{1}{N}\sum_{i=1}^{N} E_L(\vec{R}_i) \tag{38}$$

3 Algorithm

In this chapter we describe the algorithm of our DMC simulation. The simulation was carried out using the MATLAB numerical calculation environment using the MATLAB language. All random numbers was generated using MATLAB's random number generating functions "*rand*" and "*randn*" respectively for uniform and Gaussian distributions. The simulation is run multiple times in order estimate the statistical variance of the calculated energy. A flow diagram of the algorithm is shown in figure 2. Each block preforms the tasks described below.

Setup: In this block all required data for the simulation is defined. The number of time steps and the size of these are defined in an array such that the time step for the $i'th$ move of the simulation is located the $i'th$ index. The positions of the walkers are saved in a matrix of size $(n \cdot d) \times N$. Here n is the number of electrons in a set of walkers, d is the number of physical dimensions and N is the desired number of walkers. The walkers are initially distributed uniformly in the interval $[-10; 10]$ in all dimensions in order to ensure a sufficient overlap between $\Psi(\vec{R}, 0)$ and $\Psi_0(\vec{R})$. If the simulation utilizes importance sampling the trial function is defined as a string as well as finding the gradient and laplacian and saving them as string. The initial value of the reference energy is arbitrary, since it is updated after every time step, and is for convenience set to 0. After this the simulation enters a loop, where each run corresponds to taking one time step.

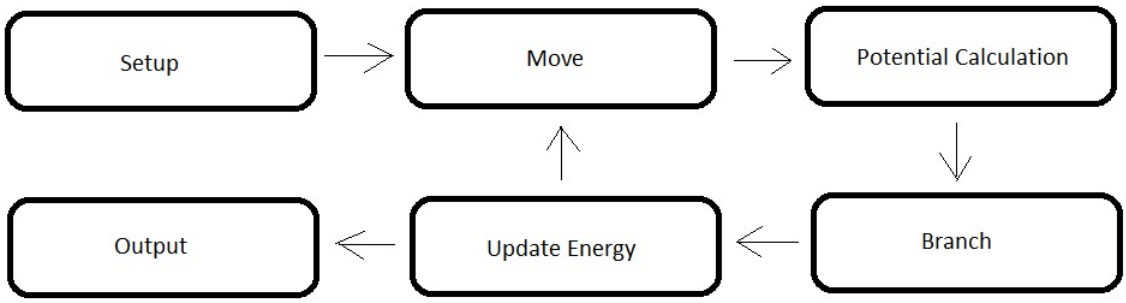

Figure 2: Flow diagram of our DMC-algorithm.

Move: Here all walkers are moved according to the earlier mentioned rules. In a simple DMC simulation without importance sampling the walkers move according to (18) in each dimension. The implementation of importance sampling add another term dependent on the drift velocity (30) to this movement.

$$\vec{x'} = \vec{x} + d\tau \cdot \vec{v}_D(\vec{R}) + \sqrt{d\tau}p \tag{39}$$

This routine also checks and ensure all walkers satisfy the fixed node approximation. This check is being done by calculating the sign of the trial wave function before and after the move. If the trial wave function changes sign the walker crossed a node and is moved back to its previous position.

Potential Calculation: This routine calculates the electronic potential or local energy of the quantum system. For the case of atoms and molecules this is done by summing all attractive and repulsive coulomb potentials present for each set of walkers.

$$V(\vec{R}) = -\sum_{ik} \frac{Z_k}{\mid \vec{r_k} - \vec{r_i} \mid} + \sum_{k_1 k_2} \frac{Z_{k_1} Z_{k_2}}{\mid \vec{r_{k_1}} - \vec{r_{k_2}} \mid} + \sum_{i_1 i_2} \frac{1}{\mid \vec{r_{i_1}} - \vec{r_{i_2}} \mid} \tag{40}$$

Since the potential might diverge for $r \longrightarrow 0$ leading to an infinite number of walkers created during the branching process there is placed a variable limit on the potential. For particles within a distance of r_c of each other the potential between them is set to the average over the volume enclosed by a shell of radius r_c.

$$\langle V \rangle = \frac{2Z_1 Z_2}{3r_c} \tag{41}$$

The value of r_c is adjusted at each time step such that the probability of birthing new walkers , P_B, has an upper limit of 1000.

$$r_c = -\frac{3}{2} \frac{1}{-\frac{log(1001)}{d\tau} + E_R} \tag{42}$$

For runs using importance sampling the local energy is calculated as.

$$E_L(\vec{R}) = -\frac{1}{2} \frac{\nabla^2 \Psi_T(\vec{R})}{\Psi_T(\vec{R})} + V(\vec{R}) \tag{43}$$

Branch: At this point we carry out the branching process of the walkers. Firstly the probabilities of walkers dying or replicating are calculated using (19), (20), (34) and (35) for simulations without and with importance

sampling. The probability of a walker dying is then compared with a random number between 0 and 1 and if higher the walker is killed off. The corresponding column in the position matrix and in the potential/local energy vector is thus removed. The probability of a walker replicating is added to a random number between 0 and 1. Each walker then replicates into a number of walkers equal to the integer part of this number. The corresponding column in the position matrix and potential/local energy vector is consequently copied into this amount of columns.

Update energy: This block calculates the average potential/local energy of the walkers, which equals the energy of the quantum system when steady state has been reached. During the first run a vector containing the average potential/local energy is generated, and this is updated each subsequent run. Hereafter the reference energy is updated according to (21).

Output: The Output block returns the results of our simulation. These are first of all the energy of the quantum system. This is the average of the energies found during steady state. Secondly it is the time evolution of energy towards the steady state and finally it is the distribution of the walkers. The density of walkers are proportional to the wave function of the quantum system.

4 Results

In this section we report the results obtained by the described algorithm generalized in $3N$ spacial dimensions, where N is the number of electrons of the quantum system. For each quantum system 40 independent calculations were made. These calculation are divided into 4 groups of 10 which terminated with different time step sizes. The details are given below. In accordance with the short time approximation the energy calculated from each of these groups are used to extrapolate the energy to $d\tau = 0$. In all calculation the total number of walkers was maintain near 1000 by updating the reference according to (21). All errors in the calculated energy exclude systematic errors and are only the statistical error determined from the variance in the energy calculated in the 10 simulations within each group.

4.1 Hydrogen

Wave functions of hydrogenic atoms are separable into a product of a radial function and a angular function, $\psi_{n,l,m}(r,\theta,\phi) = R_{n,l}(r) \cdot Y_{l,m}(\theta,\phi)$. The angular functions are known as spherical harmonic functions and the details of them and the radial functions depend on the principal quantum number, n, the orbital quantum number, l, and the magnetic quantum number. The spherical harmonic functions are complex functions except when $m = 0$. Since the DMC-method discussed above assumes real wave functions, we will stick to functions for which $m = 0$. The first 4 of these function can be seen in table 1. None of the spherical harmonics share the same nodes, and since the values of the orbital quantum number is limited to $l \leq n - 1$, we can use nodes of the spherical harmonic function corresponding to the maximum value of l when simulating a given value of n. The energy levels of hydrogen only depend on the principal quantum number. In atomic units the energy given as.

$$E_n = -\frac{1}{2n^2}$$

l	Spherical harmonic $Y_{l,0}(\theta,\phi)$
0	$\frac{1}{\sqrt{4\pi}}$
1	$\sqrt{\frac{3}{4\pi}}cos\left(\theta\right)$
2	$\sqrt{\frac{5}{16\pi}}\left(3cos^2\left(\theta\right)-1\right)$
3	$\sqrt{\frac{7}{16\pi}}\left(3cos^2\left(\theta\right)-3cos\left(\theta\right)\right)$

Table 1: The first 4 spherical harmonics for which $m = 0$

n	l	Radial wave function $R_{n,l}(r)$
1	0	$2e^{-r}$
2	1	$\frac{r}{\sqrt{24}}e^{-r/2}$
3	2	$\frac{4r^2}{81\sqrt{30}}e^{-r/3}$
4	3	$\frac{r^3}{768\sqrt{35}}e^{-r/4}$

Table 2: The first 4 radial wave functions for which the orbital quantum number has the maximum possible value.

The 4 first radial wave functions, which has the maximum possible value of the orbital quantum number is given in table 2

We see from table 1 and table 2, that the wave function of the ground state of hydrogen has no nodes, and therefore can be simulated using a simple DMC-method. For excited states, however, the radial function is zero when $r = 0$, and the number of nodes of the spherical harmonics increase with the orbital quantum number. The radial function by itself can be simulated using the simple DMC-method, since it only zero in the origin and actually do not change signs. In theory it should suffice to use the spherical harmonics as the trial wave function in importance sampled DMC simulations. In order to test this hypothesis, simulations using a product of the spherical harmonic function and a power of r as the trial wave function have been made, in addition to simulations only using the spherical harmonic. Simulations of hydrogen's first excited state without importance sampling, but instead incorporating the Cross-Recross probability (27) will also be made.

Each simulation ran for a total time of $142a.u.$. The time steps was decreased as follows: Group a) $\tau = 0-100$, $d\tau = 0.050$; $100-120$, 0.020; $120-130$, 0.010; $130-135$, 0.005; $135-137$, 0.002; $137-142$, 0.001; Group b) $0-135$, 0.050; $135-142$, 0.005; Group c) $0-130$, 0.050; $130-142$, 0.005; Group d) $0-120$, 0.050; $120-142$, 0.010. The total energy of the system was calculated by averaging the energy of the system during the last $4a.u.$. The evolution of the energy during a simple DMC-simulation of the ground state, and during an importance sampled simulation using the spherical harmonic as the trial wave function is illustrated in figure 3 and 4. All simulations employing importance sampling looked similar to figure 4, although when the trial wave function depended on r it took significantly longer for the simulation to reach the steady state. For this reason simulations of hydrogen's third excited state was increased by $100a.u.$ with a time step size of $0.05a.u.$ Also it was observed, that the energy of the system could drop very quickly before recovering, and going back towards that of the steady state. This behaviour will be discussed later. Table 3 shows the average runtimes of a single simulation.

The calculated energy for each group is illustrated in figures 5, 6, 7, and 8. A linear extrapolation to $d\tau = 0$ yields the final energy which are listed in table 4. Simulations using the Cross-Recross probability (27) returns energies significantly lower than the analytical result, suggesting the Cross-Recross probability is too low. All other results are in good agreement with the theoretical solutions, all being within two standard deviations from the exact value. Using only the spherical harmonic as the trial wave function tends to yield a better results closer to the exact value and with smaller errors. This might be explained by the laplacian of the trial wave function. The point of the local energy is, that the kinetic term, $-\nabla^2\Psi_T(\vec{R})/2\Psi_T(\vec{R})$, helps smooth the diverging behaviour of the potential as r tends to zero. For the spherical harmonics the kinetic term goes

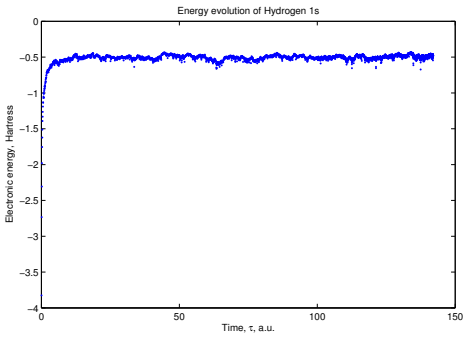

Figure 3: Evolution of the ground state energy of Hydrogen during a simple DMC simulation.

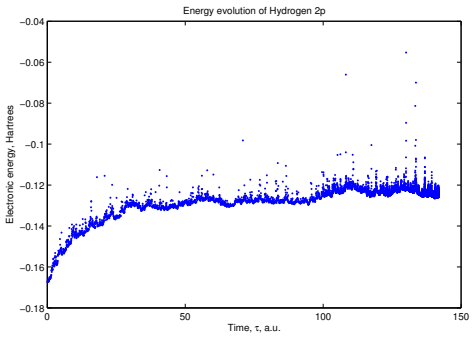

Figure 4: Evolution of the energy of Hydrogen's first excited state during an importance sampled DMC simulation using the spherical harmonic as the trial wave function.

Quantum State	Function	Runtime, sec.			
-		Group a)	Group b)	Group c)	Group d)
1s	Simple	4.20	2.15	1.68	1.55
2p	$cos(\theta)$	53.9	30.2	24.2	22.3
-	$r \cdot cos(\theta)$	15.2	8.33	6.65	6.10
-	Cross-Recross	4.98	2.60	2.05	1.88
3d	$3cos^2(\theta) - 1$	55.2	30.9	24.9	22.8
-	$r^2 \cdot (3cos^2(\theta) - 1)$	27.5	15.2	12.3	11.3
4f	$5cos^3(\theta) - 3cos(\theta)$	170	107	90.2	85.3
-	$r^3 \cdot (5cos^3(\theta) - 3cos(\theta))$	55.0	34.6	29.2	27.6

Table 3: The average runtime in seconds for one simulation.

Quantum State	Method	Function	Energy, a.u.
1s	Simple	-	$-0.495 \pm 4.10 \cdot 10^{-3}$
2p	Importance sampling	$cos(\theta)$	$-0.124 \pm 5.00 \cdot 10^{-5}$
-	Importance sampling	$r \cdot cos(\theta)$	$-0.121 \pm 2.83 \cdot 10^{-3}$
-	Cross-Recross	-	$-0.146 \pm 8.25 \cdot 10^{-4}$
3d	Importance sampling	$3cos^2(\theta) - 1$	$-0.056 \pm 5.55 \cdot 10^{-4}$
-	Importance sampling	$r^2 \cdot (3cos^2(\theta) - 1)$	$-0.058 \pm 2.67 \cdot 10^{-3}$
4f	Importance sampling	$5cos^3(\theta) - 3cos(\theta)$	$-0.031 \pm 3.10 \cdot 10^{-4}$
-	Importance sampling	$r^3 \cdot (5cos^3(\theta) - 3cos(\theta))$	$-0.033 \pm 1.17 \cdot 10^{-3}$

Table 4: The energies found by extrapolation of the simulation results to $d\tau = 0$.

towards infinity as $1/r^2$ for r going towards zero. This is faster than the potential energy so the local energy will also tend towards infinity. So instead of creating a large amount of new walkers, we simply kill off one. For the other trial functions the laplacian equals zero, so in these cases the local energy equals the potential energy, and thus is not an improvement. This would also explain the drops in energy during simulation. A walker with low potential energy has simply been replicated a large amount of times.

The final distribution of walkers are proportional to $\psi_0(\vec{R})$, or $f(\vec{R})$ in the case of importance sampling. We can therefore visualize the wave functions by plotting the density of the walkers. These are illustrated in

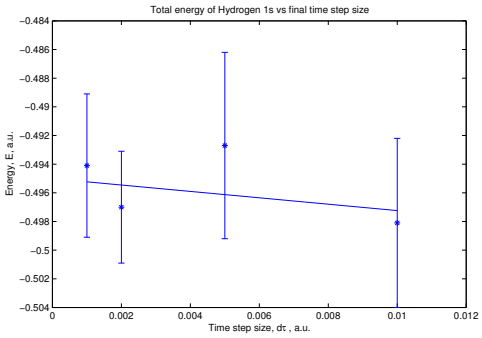

Figure 5: Variation of the total energy of hydrogen's ground state with time step size for simulations. A linear fit is used to extrapolate the energy to $d\tau = 0$.

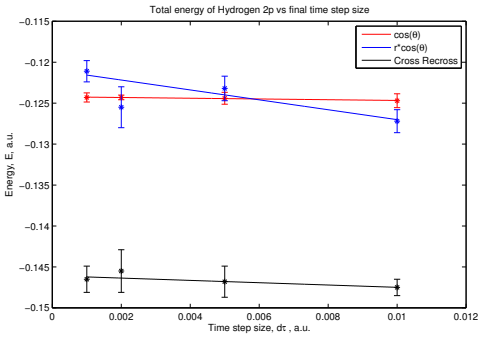

Figure 6: Variation of the total energy of hydrogen's first excited state with time step size for simulations using different trial wave function (red/blue) and simulations using the Cross-Recross probability. A linear fit is used to extrapolate the energy to $d\tau = 0$.

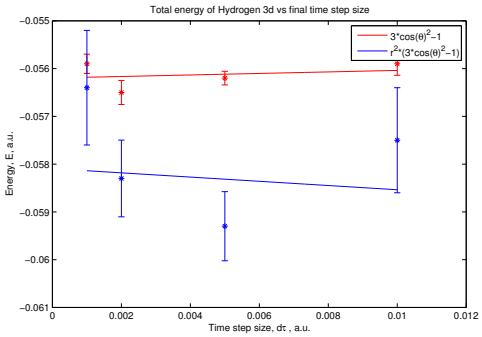

Figure 7: Variation of the total energy of hydrogen's second excited state with time step size for simulations using different trial wave function. A linear fit is used to extrapolate the energy to $d\tau = 0$.

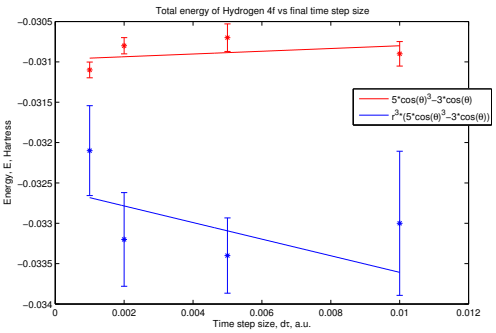

Figure 8: Variation of the total energy of hydrogen's third excited state with time step size for simulations using different trial wave function. A linear fit is used to extrapolate the energy to $d\tau = 0$.

figures 9-16 for simulation using only the spherical harmonics as the trial wave function. Since the spherical harmonics are independent of r, the radial part of $f(\vec{R})$ are equal to the radial part of $\psi_0(\vec{R})$. Therefore it is not necessary to compensate for the trial wave function. The final radial distribution of $f(\vec{R})$ was very different from the exact wave function when the trial function had a radial dependence. For small values of r, it appears the distribution does not match the exact radial function, but overall the radial distribution of walkers are fairly accurate. The angular distribution also fit the analytical result very well. The apparent gap along the z-axis in figure 13 and figure 15 are due to an error in the representation, that made this region sparsely populated. There are, however, some walkers present in contrast to the completely empty regions along the nodal lines, indicated by green lines.

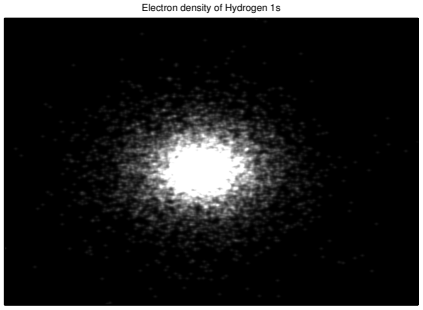

Figure 9: The final distribution of walkers in the xz-plane from a simple DMC simulation of the hydrogen ground state. The walkers are all located near the origin in a sphere corresponding to the $1s$ orbital.

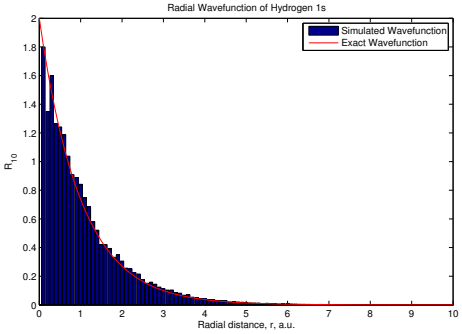

Figure 10: The final radial distribution of walkers from a simple DMC-simulation of the hydrogen ground state. The exact radial wave function is given in red.

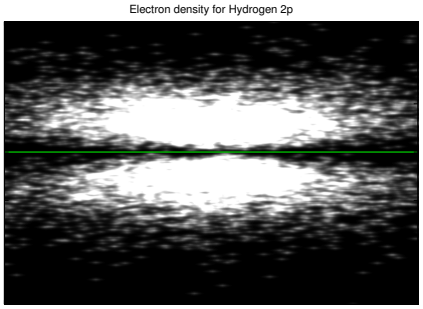

Figure 11: The final distribution of walkers in the xz-plane from a DMC simulation of hydrogen's first excited state. The walkers are all located in two bulges along the z-axis corresponding to the $2p_z$ orbital. The green line indicate the node of the spherical harmonic.

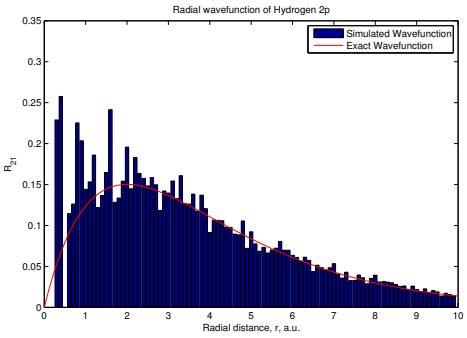

Figure 12: The final radial distribution of walkers from a DMC-simulation of hydrogen's first excited state. The exact radial wave function is given in red.

4.2 Helium

Several very accurate variational calculations have been made on the Helium atom. These have calculated the energy of the ground state configuration $1s^2$ to be $E_{1s^2} = -2.903724377034119598 13a.u.$ which is identical to the experimental exact value. Since the electrons have opposite spin the wave function for this configuration is space-symmetric and we can therefore assume it is positive definite making this configuration eligible for a simple DMC simulation. For the Helium atom each simulation ran for a total time of $48.5a.u.$. The time steps was decreased as follows: Group a) $\tau = 0 - 25$, $d\tau = 0.050$; $25 - 35$, 0.020; $35 - 40$, 0.010; $40 - 42.5$, 0.005; $42.5 - 43.5$, 0.002; $43.5 - 48.5$, 0.001; Group b) $0 - 42.5$, 0.050; $42.5 - 48.5$, 0.005; Group c) $0 - 40$, 0.050; $40 - 48.5$, 0.005; Group d) $0 - 35$, 0.050; $35 - 48.5$, 0.010. The total energy of the system was calculated by averaging the energy of the system during the time interval $44.5 - 48.5$. The evolution of the energy was similar in all runs and is illustrated in figure 17. The calculated energy for each group is illustrated in figure

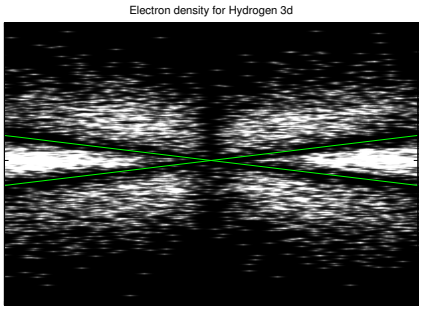

Figure 13: The final distribution of walkers in the xz-plane from a DMC simulation of hydrogen's second excited state. The walkers are all located away from the nodes of the spherical harmonic, indicated by the green lines.

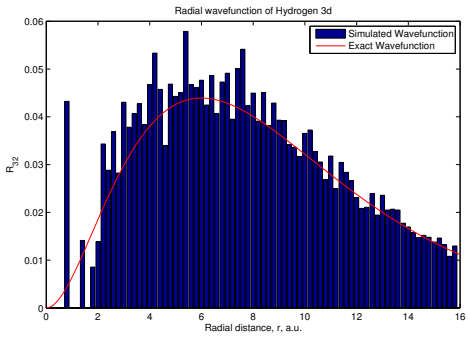

Figure 14: The final radial distribution of walkers from a DMC-simulation of hydrogen's second excited state. The exact radial wave function is given in red.

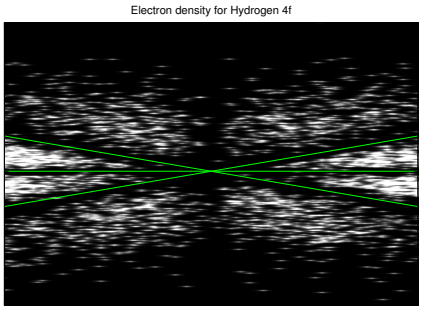

Figure 15: The final distribution of walkers in the xz-plane from a DMC simulation of hydrogen's third excited state. The walkers are all located away from the nodes of the spherical harmonic, indicated by the green lines.

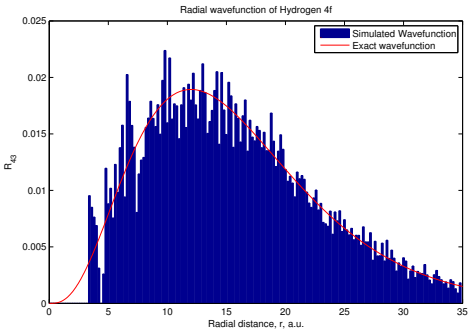

Figure 16: The final radial distribution of walkers from a DMC-simulation of hydrogen's third excited state. The exact radial wave function is given in red.

18. A linear extrapolation to $d\tau = 0$ yields the final energy of.

$$E = -2.900 a.u. \pm 0.030 a.u.$$

This is in good agreement with the exact result. The final distribution of the walkers as seen on figure 19 is clumped around the origin consistent with both electrons being in the $1s$ orbital. The average runtime for the simulations in group a was 4.06 seconds, while the groups took $2.04s$ for group b, $1.33s$ for group c and $1.11s$ for group d.

The first excited state of Helium, $1s2s$, is the lowest space-antisymmetric state. Using variational calculations for the space-antisymmetric Helium $1s2s$ configuration a wave function consisting of a simple Slater-determinant have been calculated.

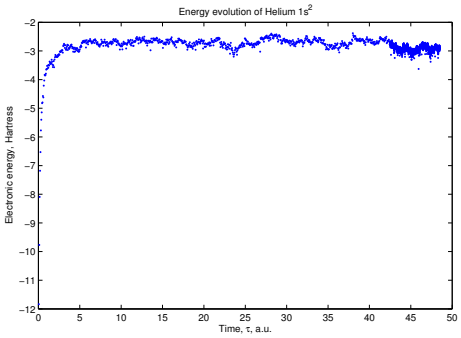

Figure 17: Evolution of the electronic energy of Helium $1s^2$ during a simple non-importance sampled DMC simulation.

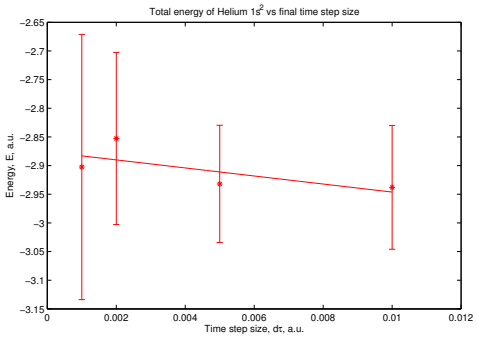

Figure 18: Variation of the total energy of Helium $1s^2$ with time step size. A linear fit is used to extrapolate the energy to $d\tau = 0$.

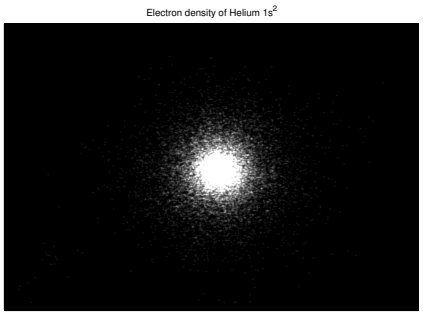

Figure 19: The final distribution of walkers in the xz-plane from a simple DMC simulation of the Helium $1s^2$ configuration. All walkers are located around the origin consistent with the electrons being in the $1s$ orbital.

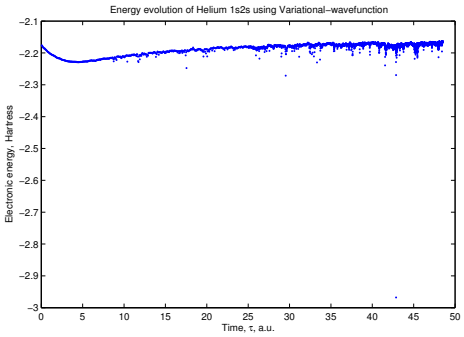

Figure 20: Evolution of the electronic energy of Helium $1s2s$ during an importance sampled DMC simulation using a trial wave function optimized using variational calculations.

$$\Phi = e^{-2.01\vec{r}_1}\left(1 - \frac{1.53\vec{r}_2}{2}\right)e^{-1.53\vec{r}_2/2} - e^{-2.01\vec{r}_2}\left(1 - \frac{1.53\vec{r}_1}{2}\right)e^{-1.53\vec{r}_1/2} \tag{44}$$

The energy corresponding with this wave function is $E_{1s2s} = -2.167a.u.$ which is in good agreement with the results from more elaborate trial wave function using Hylleraas coordinates. This simple Slater-determinant equals zero only when $\vec{r}_1 = \vec{r}_2$. Therefore $\Phi = \vec{r}_1 - \vec{r}_2$ might be a simple trial wave function for importance sampled simulations of Helium $1s2s$. Importance sampled DMC simulations using both (44) and the more simple $\Phi = \vec{r}_1 - \vec{r}_2$ as the trial wave function has been made. The evolution of the energy for both trial wave functions are pictured in figure 20 and 21. We see that at steady state the energy in simulations using the simple wave function are more varying, which also can be seen from the significantly larger errors in the energies from the simple trial wave function simulations in figure 22. The energy found by linear extrapolation if.

$$E_{variational} = -2.176a.u. \pm 2.750 \cdot 10^{-3}a.u.$$

$$E_{simple} = -2.170a.u. \pm 9.000 \cdot 10^{-3}a.u.$$

Both of these energies are within one standard deviation of the exact energy $E_e x = -2.175a.u.$ calculated from elaborate Hylleraas-wave functions. The simple wave function, however, does produce increased statistical errors but the runtime of the simulations were on average 8.32 times faster than the simulations using the variational optimized wave function.

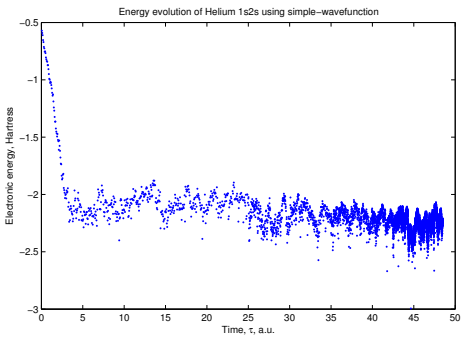

Figure 21: Evolution of the electronic energy of Helium $1s2s$ during an importance sampled DMC simulation using a simple trial wave function.

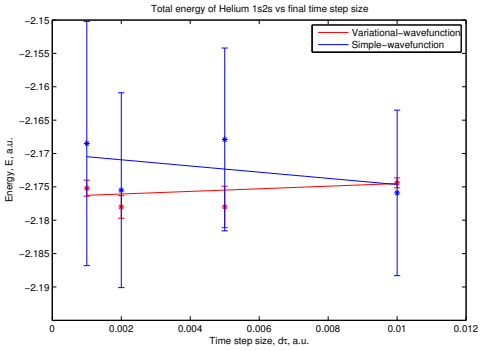

Figure 22: Variation of the total energy of Helium $1s2s$ with time step size for simulations using an optimized trial wave function (red) and a simple trial wave function (blue). A linear fit is used to extrapolate the energy to $d\tau = 0$.

In figure 23 and 24 the final walker distribution in the xz-plane is pictured. In figure 23 both the $1s$ and $2s$ orbitals are clearly visible, but in figure 24 only the $1s$ is clear. The rest of the electrons apart for some outliers are concentrated in a shell like structure around the densely packed sphere, but they are more scattered unlike the clear spherical shell in figure 23. It looks as if the simple trial function does not give a precise image of the wave function, although the symmetry is apparent.

4.3 H^-

For the H^- ion each simulation ran for a total time of $192a.u.$. The time steps was decreased as follows: Group a) $\tau = 0 - 150$, $d\tau = 0.050$; $150 - 170$, 0.020; $170 - 180$, 0.010; $180 - 185$, 0.005; $185 - 187$, 0.002; $187 - 192$, 0.001; Group b) $0 - 185$, 0.050; $185 - 192$, 0.005; Group c) $0 - 180$, 0.050; $180 - 192$, 0.005; Group d) $0 - 170$, 0.050; $170 - 192$, 0.010. The total energy of the system was calculated by averaging the energy of the system during the time interval $188 - 192$. As with the ground state of the Helium atom the wave function of the ground state of H^- is space-symmetric and a simple non importance sampled simulation is sufficient. The evolution of the energy was similar to the evolution in the Helium ground state. The calculated energy for the four groups and their statistical variance are pictured in figure 25. Extrapolation to $d\tau = 0$ yields the energy

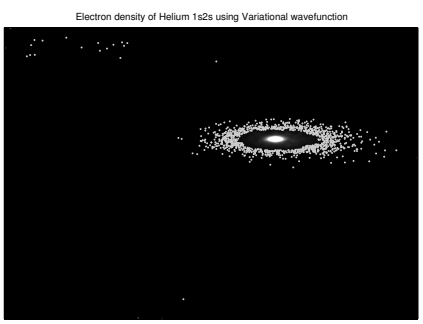

Figure 23: The final distribution of walkers in the xz-plane from a DMC simulation of the Helium $1s2s$ configuration using an optimized trial wave function. The walker are apart from a few outliers clearly separated in a sphere close to the origin surrounded by a spherical shell corresponding to the $1s$ and $2s$ orbitals.

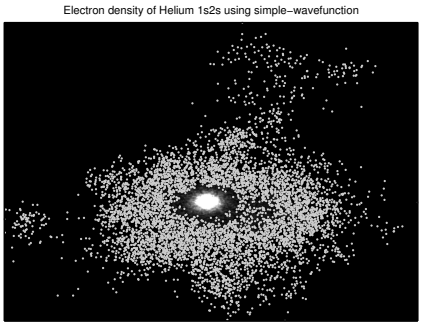

Figure 24: The final distribution of walkers in the xz-plane from a DMC simulation of the Helium $1s2s$ configuration using a simple trial wave function. Most walkers are located in a sphere around the origin corresponding to the $1s$ orbital, however a spherical shell corresponding to the $2s$ orbital is not clearly visible.

$E_{1s^2} = -0.5251a.u. \pm 6.175 \cdot 10^{-3}a.u.$ in good agreement with the experimental value $E_{ex} = -0.528a.u$. The distribution of walkers illustrated in figure 26 are also in agreement with both electrons being in the $1s$ orbital.

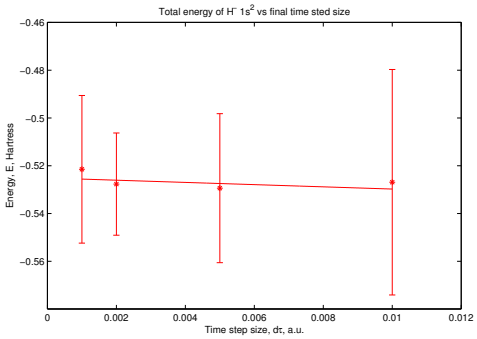

Figure 25: Variation of the total energy of H^- $1s^2$ with time step size. A linear fit is used to extrapolate the energy to $d\tau = 0$.

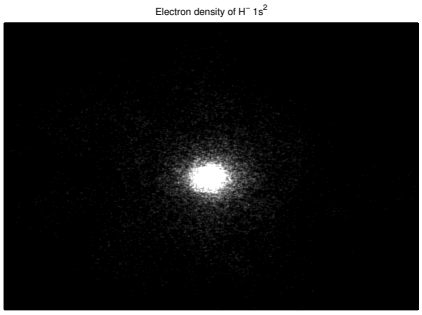

Figure 26: The final distribution of walkers in the xz-plane from a simple DMC simulation of the H^- $1s^2$ configuration. All walkers are located around the origin consistent with the electrons being in the $1s$ orbital.

Using the same simple trial wave function $\Phi = \vec{r_1} - \vec{r_2}$ as we used when calculating the first excited state of Helium, we will try to calculate a potential excited state of H^-. The evolution of the energy illustrated in figure 27 are again similar to the simulations of Helium, and the errors in the energy as seen on 28 are of a relative same size being approximately 1% of the calculated energy. The energy found by extrapolation to $d\tau = 0$ is $E = -0.5041a.u. \pm 7.175 \cdot 10^{-3}a.u.$. This is within one standard deviation of the ground state of Hydrogen in agreement with experimental results that, the negative ion H^- only has one bound state with a very small ionization potential. The final walker distribution in figure 29 also indicate an empty $2s$ orbital. Most electrons are located near the nucleus, however, the remaining electrons are not located in a

clear surrounding ring as was the case for the Helium atom. Our simulations therefore indicate a single bound state with the ionization potential $I_p = 0.0210 a.u. \pm 9.466 \cdot 10^{-3}$. This is a bit lower but still within one standard deviation from the experimental value $I_p^{exp} = 0.0286 a.u.$.

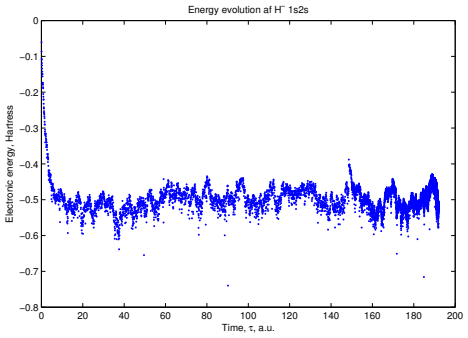

Figure 27: Evolution of the electronic energy of H^- $1s2s$ during an importance sampled DMC simulation using a simple trial wave function.

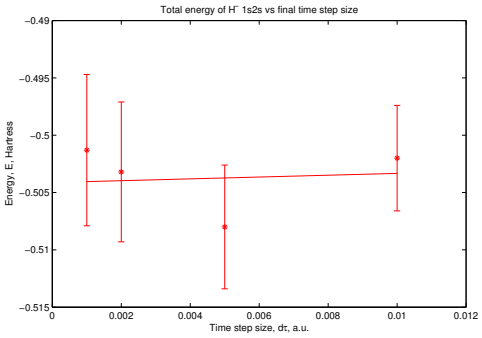

Figure 28: Variation of the total energy of H^- $1s2s$ with time step size. A linear fit is used to extrapolate the energy to $d\tau = 0$

4.4 H_2^+

When studying molecules the usual starting point is the linear combination of atomic orbitals (LCAO). So lets try to reproduce these results. H_2^+ is a homonuclear diatomic molecule, and therefore has a point of symmetry on the internuclear axis in the middle of the nuclei. Electronic wave functions can thus be classified according to the parity under reflection with respect to this point. A simulation of the lowest even state, called gerade, should not require a trial wave function, while the lowest odd state, called ungerade, would require a trial wave function, which changes sign when reflected though the middle point between the nuclei. If we

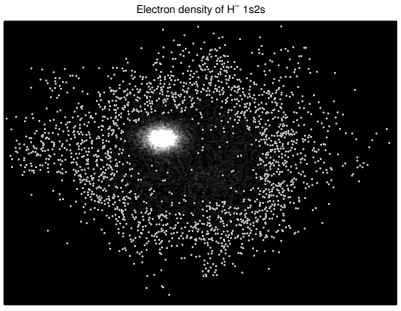

Figure 29: The final distribution of walkers in the xz-plane from a DMC simulation of the h^- $1s2s$ configuration using a simple trial wave function. Most walkers are located in a sphere around the origin corresponding to the $1s$ orbital. The remaining walkers scattered in space with any systematic distribution.

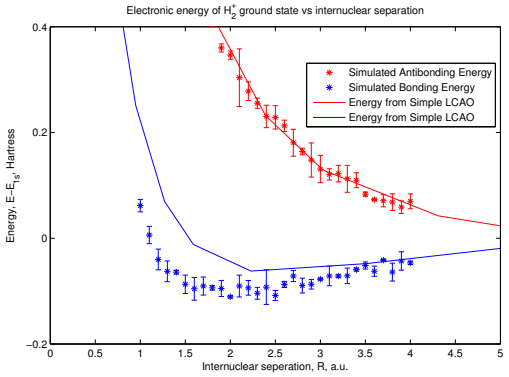

Figure 30: The electronic potential curves of the lowest gerade (blue) and ungerade (red) state of H_2^+. The energy of the ungerade state is positive for all internuclear distance, meaning no molecule can be formed in this state. The energy of the gerade state exhibits a negative minimum at $R = 2a.u.$ meaning, this states leads to bonding between the two nuclei.

place the internuclear axis along the z-axis and the middle point at the origin, a simple such function would be $g = z$. Each simulation ran a total of $142a.u.$ with the same time steps as hydrogen. Figure 30 shows the energy found by extrapolation to $d\tau = 0$ offset by the ground state energy of hydrogen as a function of the internuclear distance. These curves are known as electronic potential curves. The blue data are the energies of the gerade-state and the red the energies of the ungerade state. We see that the energy of the ungerade state are positive for all internuclear distances, meaning this state is repulsive for all distances and does not lead to bonding between the nuclei. A molecule in this state would instantly separate into a proton and a hydrogen atom. This state is called the antibonding state. On the other hand the gerade state shows negative energies, meaning that there is an attraction leading to a stable molecule. This state is called a bonding state. The minimum is located at internuclear separation of $2a.u.$ and attains the value $-0.111a.u. \pm 2.00 \cdot 10^{-3}$. Overall the calculated energies of the gerade state are lower then the energies found by simple LCAO. However, very accurate numerical solutions of the Schrödinger electronic equation have shown the energies of the bonding state predicted by LCAO are slightly to high, in agreement with our result. Moreover the numerical solutions predict the minimum to be $-0.103a.u.$ at a separation distance of $2.00a.u.$ also in agreement with our results.

The bonding and antibonding of the states can also be seen in figure 31 and 32, which shows the final walker distribution in the xz-plane. The grade state has a large number of walkers located between the nuclei, indicating the wave function is large in this region, and the electron is shared by the nuclei. Meanwhile the region is empty in the ungerade state, indicating the wave function is close to zero, and the electron is bound to only one nuclei.

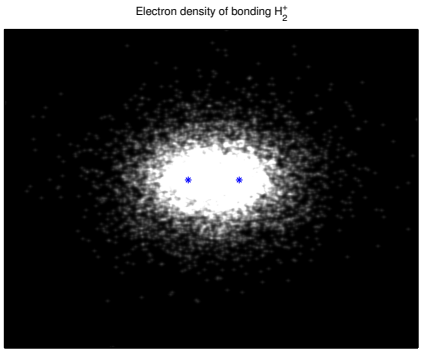

Figure 31: The final walker distribution in a simple DMC-simulation of H_2^+. This distributes the walkers according to the lowest gerade state, leading to a bonding between the nuclei. This can be seen by the large amount of walkers between the two nuclei.

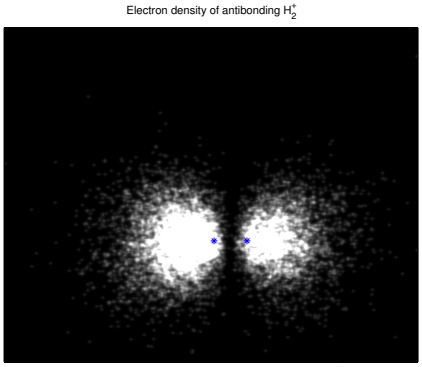

Figure 32: The final walker distribution in a DMC-simulation of H_2^+ using $g = z$ as a trial wave function. This distributes the walkers according to the lowest ungerade state, leading to an antibonding between the nuclei. This can be seen by the gap in walkers between the two nuclei.

5 Conclusion

In this paper, a detailed account of the theoretical background for the diffusion Monte Carlo method for solving the Schrödinger equation has been presented. The importance of the trial wave function in importance sampled DMC-simulations have been studied through simulations of few-body systems. We found, that simple trial wave functions are useful for finding a rough estimation of the energy expectation values with a minimal of computation effort. Simple trial wave functions are, however, not useful for finding the precise wave function since the final walkers are distributed according to the product $\Psi_T(\vec{R})\Psi_0(\vec{R})$, but can be useful for illustrating the symmetry. For a more accurate value of the energy and a precise picture of the wave function it is necessary to use a trial function optimized by some other means at the cost of increased computation time. The DMC-method seems to be most suited for systems with several electrons since it does not require the usage of complicated multidimensional integrals, basis sets, or large matrices like other numerical methods. For these larger systems the importance of the trial wave function might increase due to the more complicated structure of the nodal planes. The discussed method assumes real wave functions, so a natural step would be to generalise the method to complex wave functions.

Bibliography

[1] Paul Richard Charles Kent: *Techniques and Applications of Quantum Monte Carlo*, http://www.physics.uc.edu/~pkent/thesis/Thesis.html

[2] W.M.C. Foulkes, L. Mitas, R.J. Needs, G. Rajagopal: *Quantum Monte Carlo simulations of solids*, Reviews of Modern Physics 74(1), 33, (2001)

[3] James B. Anderson: *A random-walk simulation of the Schrödinger equation:* H_3^+, J. Chem. Phys. 63(4), 1499, (1975)

[4] James B. Anderson: *Quantum chemistry by random walk.* $H\ ^2P$, $H_3^+\ D_{3h}\ ^1A_1$, $H_2\ ^3\Sigma_u^+$, $H_4\ ^1\Sigma_g^+$, $Be\ ^1S$, J. Chem. Phys. 65(10), 4121, (1976)

[5] Ioan Kosztin, Byron Faber, Klaus Schulten: *Introduction to the Diffusion Monte Carlo Method* http://www.thphys.uni-heidelberg.de/~wetzel/qmc2006/KOSZ96.pdf

[6] Wikipedia entry on Monte Carlo integration. http://en.wikipedia.org/wiki/Monte_Carlo_integration

[7] David J. Griffiths: Introduction to Quantum Mechanics (International edition), 2. edition, Pearson Education, (2005)

[8] B.H. Brandsen, C.J. Joachain: Physics of Atoms and Molecules, 2. edition, Pearson Education, (2003)

A Modification of the Schrödinger Equation

We will show the deviation of the importance sampled Schrödinger equation (28). The following two vector calculus identities are considered known, and will be used without proof.

$$\nabla(\Psi(\vec{R},\tau)\cdot\nabla\phi(\vec{R})) = \Psi(\vec{R},\tau)\cdot\nabla^2\phi(\vec{R}) + \nabla\Psi(\vec{R},\tau)\cdot\nabla\phi(\vec{R})$$

$$\nabla^2(\Psi(\vec{R},\tau)\phi(\vec{R})) = \phi(\vec{R})\cdot\nabla^2\Psi(\vec{R},\tau) + \Psi(\vec{R},\tau)\cdot\nabla^2\phi(\vec{R}) + 2\nabla\Psi(\vec{R},\tau)\cdot\nabla\phi(\vec{R})$$

Multiplying the imaginary time Schrödinger equation in atomic units (9) by a trial wave function $\phi(\vec{R})$ yields.

$$\begin{aligned}
-\frac{\delta f(\vec{R},\tau)}{\delta\tau} = -\frac{\delta\Psi(\vec{R},\tau)}{\delta\tau}\phi(\vec{R}) &= -\frac{1}{2}\phi(\vec{R})\nabla^2\Psi(\vec{R},\tau) + (V(\vec{R}) - E_R)f(\vec{R},\tau) \\
&= -\frac{1}{2}\phi(\vec{R})\nabla^2\Psi(\vec{R},\tau) - \frac{1}{2}\Psi(\vec{R},\tau)\cdot\nabla^2\phi(\vec{R}) - \nabla\Psi(\vec{R},\tau)\cdot\nabla\phi(\vec{R}) \\
&+ \frac{1}{2}\Psi(\vec{R},\tau)\cdot\nabla^2\phi(\vec{R}) + \nabla\Psi(\vec{R},\tau)\cdot\nabla\phi(\vec{R}) + (V(\vec{R}) - E_R)f(\vec{R},\tau) \\
&= -\frac{1}{2}\nabla^2 f(\vec{R},\tau) + \frac{1}{2}\Psi(\vec{R},\tau)\cdot\nabla^2\phi(\vec{R}) + \nabla\Psi(\vec{R},\tau)\cdot\nabla\phi(\vec{R}) + (V(\vec{R}) - E_R)f(\vec{R},\tau) \\
&= -\frac{1}{2}\nabla^2 f(\vec{R},\tau) + \Psi(\vec{R},\tau)\cdot\nabla^2\phi(\vec{R}) + \nabla\Psi(\vec{R},\tau)\cdot\nabla\phi(\vec{R}) \\
&- \frac{1}{2}\Psi(\vec{R},\tau)\cdot\nabla^2\phi(\vec{R}) + (V(\vec{R}) - E_R)f(\vec{R},\tau) \\
&= -\frac{1}{2}\nabla^2 f(\vec{R},\tau) + \nabla(\Psi(\vec{R},\tau)\cdot\nabla\phi(\vec{R})) - \frac{1}{2}\Psi(\vec{R},\tau)\cdot\nabla^2\phi(\vec{R}) + (V(\vec{R}) - E_R)f(\vec{R},\tau) \\
&= -\frac{1}{2}\nabla^2 f(\vec{R},\tau) + \nabla\left(f(\vec{R},\tau)\cdot\frac{\nabla\phi(\vec{R})}{\phi(\vec{R})}\right) - \frac{1}{2}f(\vec{R},\tau)\cdot\frac{\nabla^2\phi(\vec{R})}{\phi(\vec{R}} + (V(\vec{R}) - E_R)f(\vec{R},\tau) \\
&= -\frac{1}{2}\nabla^2 f(\vec{R},\tau) + \nabla\left(f(\vec{R},\tau)\cdot\frac{\nabla\phi(\vec{R})}{\phi(\vec{R})}\right) + \left(-\frac{1}{2}\frac{\nabla^2\phi(\vec{R})}{\phi(\vec{R})} + V(\vec{R}) - E_R\right)f(\vec{R},\tau) \\
&= -\frac{1}{2}\nabla^2 f(\vec{R},\tau) + \nabla(\vec{v}_D f(\vec{R},\tau)) + (E_L(\vec{R}) - E_R)f(\vec{R},\tau)
\end{aligned}$$